Aquatic Mammals 2015, *41*(4), 434-443, DOI 10.1578/AM.41.4.2015.434

The Maskogram: A Tool to Illustrate Zones of Masking

Christine Erbe

Centre for Marine Science & Technology, Curtin University, PO Box U1987, Perth, WA 6845, Australia
E-mail: c.erbe@curtin.edu.au

Abstract

The prediction of masking in marine mammals is most commonly based on the power spectrum model of masking and the concept of equal power of signal and noise at the detection threshold, within the auditory filter centred at the peak of the signal. While this model works well for narrowband signals embedded in broadband noise, it fails in many realistic listening scenarios. In this paper, a visualisation tool, called a maskogram, is presented that illustrates the extent of the zone of masking around a noise source and with which the effects of various parameters and anti-masking mechanisms can be examined. A series of maskograms is presented based on behavioural experiments with a beluga whale (*Delphinapterus leucas*) for which the signal was a recorded beluga call and the noise was recorded from an icebreaker. Certain masking release mechanisms, such as comodulation masking release, within-valley listening, and multiple looks, likely occurred during the behavioural experiments and are indirectly included in the data feeding into the maskograms. The effects of a spatial release from masking are illustrated based on data from other species, signals, and noise. Studies with realistic signals and noise are needed to show the limitations of the existing models, to determine masking in real-world situations, to better understand masking release mechanisms, and to ultimately improve models of masking.

Key Words: masking, zone of masking, critical ratio, power spectrum model of masking

Introduction

Underwater noise can have a number of effects on marine mammals (see Richardson et al., 1995, for a comprehensive review or Erbe, 2012, for a brief and more recent summary), including modification of behaviour, hearing threshold shift(s), stress, and masking. Masking is likely an important, yet largely undocumented consequence of underwater noise. Sound supports many life functions of marine mammals. Marine mammals communicate acoustically during a variety of behaviours, including travelling, feeding, mating, and nursing (e.g., Herzing, 1996; Tyack, 1998). Marine mammals likely use environmental sounds for navigation and orientation, although this remains to be proven. They listen to the sounds of prey for feeding (Gannon et al., 2005) and to the sounds of predators for avoidance (Cure et al., 2013). In addition, odontocetes have a biosonar system for active echolocation to investigate the subsea environment and to find prey (Au, 1993).

The ocean is naturally noisy with abiotic noise from wind, waves, precipitation, ice break-up, and so on, and biotic noise from whales, fish, crustaceans, and so on. Underwater noise, whether of natural or anthropogenic origin, can interfere with the detection and comprehension of these sounds, a phenomenon called masking. Masking has been studied in several odontocete and pinniped species in captive settings, using behavioural experiments or auditory evoked potential measurements (e.g., Johnson, 1968; Johnson et al., 1989; Turnbull & Terhune, 1990; Southall et al., 2000; Kastelein et al., 2009; Gaspard et al., 2012; Ghoul & Reichmuth, 2014). Masking studies are commonly designed to measure a specific parameter or process relevant to signal detection or masking, such as parameters of the auditory filter. In order to isolate one parameter or variable for study, these experiments typically include synthetic and simple signals (e.g., pure tones) and noise (e.g., white noise). Studies with complex signals and/or noise are rare (Erbe & Farmer, 1998; Erbe, 2000; Lucke et al., 2007; Branstetter & Finneran, 2008; Trickey et al., 2010; Kastelein et al., 2011; Branstetter et al., 2013a; Cunningham et al., 2014) due to the fact that it is difficult (1) to explain the observations when multiple, simultaneous variables are involved; (2) to derive parameters that could improve models of masking; (3) to generalise the results; and (4) to apply the results to the prediction of masking in scenarios with signals, noise, and species other than the very specific combination(s) measured.

Predictions of masking usually rely on the power spectrum model of masking, which was developed for humans and which approximates the auditory system by a series of overlapping bandpass filters (Fletcher, 1940; Moore, 1995). When exposed to a signal embedded in noise, each filter receives signal and noise power at a certain signal-to-noise ratio (SNR), which depends on the spectral characteristics of the signal and noise. Detection of a signal is assumed to be determined by the filter with the highest SNR. If the signal is of tonal character, this will be the filter centred on the tone frequency. Only noise that passes through the same bandpass filter is considered effective at masking the signal. Whether signal detection is successful depends on the SNR at this filter. Fletcher (1940) further postulated that at detection threshold, the powers of signal and noise within the auditory filter surrounding the signal are equal (SNR = 0 dB). In the case of a tone being masked by broadband white noise, the ratio of the tone power (Pt) and the noise power spectral density (PSDn, power per Hz) at detection threshold is called the critical ratio (CR). It is typically expressed in decibels as $CR = 10\log_{10}(Pt/PSDn) = 10\log_{10}(Pt) - 10\log_{10}(PSDn)$—that is, the CR is level difference between the signal power and the noise power spectral density. It can be converted to a measure of bandwidth, called the critical band ($CB = 10^{CR/10}$); however, the agreement between the CB computed this way and the width of the underlying auditory filters measured with maskers of variable bandwidth can be poor (Au & Moore, 1990; Southall et al., 2003). The CR has been shown to be a powerful predictor for masking in many listening scenarios in birds (Dooling & Blumenrath, 2014).

There are many simplifying assumptions underlying the power spectrum model of masking—ignoring, for example—that information from multiple filters can be combined to enhance signal detection, that noise from outside the signal band can add to the masking, that the filter width is level-dependent to some extent, and that signal and noise often have temporal structures that are not captured in this model (Moore, 1995). There are additional releases from masking that cannot be explained by the power spectrum model of masking. If the masker is amplitude modulated across a number of auditory filters, the listener's auditory system can correlate the output from different filters to determine when the signal occurs. This is termed *comodulation masking release* and has been demonstrated in a few marine mammals (Branstetter & Finneran, 2008; Erbe, 2008; Trickey et al., 2010; Branstetter et al., 2013b; Cunningham et al., 2014). If the masker and the signaller are spatially separated (i.e., the sounds arrive at the listener from different directions), a spatial release from masking due to binaural hearing might additionally enhance signal detection. With separations of up to 180° in the horizontal plane, the amount of masking varied as a function of angle by up to 19 dB at frequencies of 1 to 18 kHz (Zaitseva et al., 1975, 1980; Bain & Dahlheim, 1994; Turnbull, 1994; Holt & Schusterman, 2007; note that Holt & Schusterman, 2007, studied pinnipeds in air, whereas the others studied cetaceans and pinnipeds under water).

It is difficult to generalize these results and to incorporate them in a general masking model that will apply to realistic and complex listening scenarios. In this paper, a visualisation tool (rather than a model) is presented that can illustrate the effect of some of these processes on the resulting zone of masking.

The Maskogram

A simple way of visualising zones of masking is to take a bird's-eye view (Figure 1), imagine the sound footprints of the masker (e.g., a ship) and the signal (e.g., a whale sound), and look for overlap. A listener can be anywhere in the figure. In the area of overlap, depending on the spectral and temporal characteristics of the masker and signal, either one or the other, or both, might be audible to a listener. Assuming a continuous masker and a tonal signal, and using the power spectrum model of masking and CR data for the listening species, the signal would be audible in the area of overlap

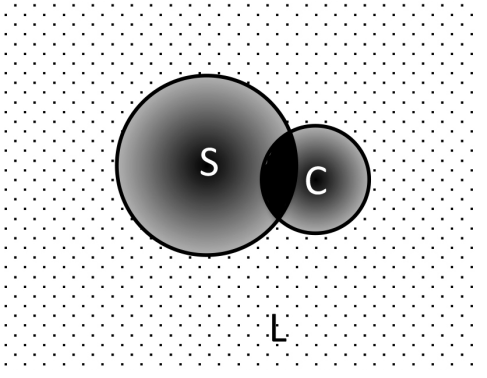

Figure 1. Bird's-eye view of a zone of masking created by a ship (S) near a calling whale (C). The audible sound footprints of the ship and the calling whale are indicated by the grey shaded circles, with highest received levels in the centres. The listening whale (L) can be anywhere. Outside both circles S and C, the listener hears neither ship nor whale. Inside circle S, the ship is audible; inside circle C, the whale is audible. In the black area of overlap, some masking might occur depending on the spectral levels of signal and noise.

if the level difference between signal power and masker power spectral density exceeded the CR; otherwise, it would be masked.

The shape and size of the area of overlap (i.e., the shape and size of the potential zone of masking in real-life situations) change as the positions of the masker and the caller change, and it is clumsy to quantify the masking potential over all possible combinations of positions. In the power spectrum model of masking, only the received levels of masking noise and signal matter, and these are determined by the ranges between the listener and the masker and between the listener and the caller. [**Note:** Being classified as the "caller" does not imply the animal is calling another, but, rather, that it is emitting a communication signal.] One way of illustrating the variable extent of the potential zone of masking as a function of the relative positions of caller, listener, and masker is the so-called maskogram in which these ranges are plotted against each other.

The following maskograms are illustrated with data from a masked hearing experiment with a captive, trained beluga whale at Vancouver Aquarium, Canada (Erbe & Farmer, 1998; Erbe, 2000). The animal had been trained to position itself with the tip of its rostrum touching a pole mounted in front of an underwater sound projector as an indication that it was prepared to begin a sound exposure trial. A beluga sound (referred to as a *call*) was played as the signal upon which the animal had been trained to leave the pole and touch a response pole at the opposite side of the pool.

The 1.6-s call had been recorded from a wild, Arctic population and consisted of six 150-ms-long emissions of an 800-Hz tone with harmonic and nonharmonic overtones up to 8 kHz (see Figure 1 in Erbe, 2000). Four types of masking noise were played through the same sound projector: (1) an icebreaker's bubbler system noise, (2) an icebreaker's propeller cavitation noise, (3) naturally occurring thermal ice-cracking noise, and (4) artificially created Gaussian white noise. Ice-cracking noise consisted of sharp (< 100 ms) broadband pulses with most energy below 5 kHz. Propeller cavitation noise was broadband (32 Hz to 22 kHz) and strongly amplitude-modulated by the 11-Hz blade rate. Bubbler system noise was similarly broadband and continuous with a weak amplitude modulation of 2 Hz as a result of injecting bubbles into the ocean twice per second. Gaussian white noise had a flat spectrum up to 22 kHz and was temporally continuous.

The beluga call was inserted into the noise at a fixed phase (Erbe & Farmer, 1998) and randomly (Erbe, 2000). In other words, in the former case, the call always happened at the same time in the noise; while in the latter case, the call happened at a random time in the noise, and the pulses of the call were shifted randomly against the pulses of the noise. The relative levels of signal and noise were altered during the trials, and catch trials (noise only) were inserted to reinforce the animal's stationing behaviour and to compute receiver-operating characteristics (Erbe & Farmer, 1998). Detection thresholds, expressed as *critical SNR* (computed over the bandwidth of the call, 800 Hz to 8 kHz), were determined statistically as the mean over all of the phase shifts between call and noise.

A noise-centred maskogram shows the zones of predicted masking around a noise source as a function of distances to a calling animal and to a listening animal. The general layout of a maskogram is explained in Figure 2 (top). As a first step, it helps to imagine a ship being located along the y-axis. The range from the ship increases along the positive x-axis. The colours represent the broadband (32 Hz to 22 kHz) received level (RL) of the ship with a source level (SL) of 192 dB re 1 µPa @ 1 m. To model propagation loss, a combination of spherical (until the range equalled the water depth) and cylindrical spreading (for ranges greater than the water depth) was used with molecular absorption (Ainslie & McColm, 1998).

Other, more sophisticated sound propagation models can easily be incorporated with a maskogram. Power spectra were computed for the call and noises and were propagated until the call level reached the detection threshold of the call in quiet conditions (in the absence of experimental noise and with all machinery around the pool switched off) as measured behaviourally (Erbe & Farmer, 1998) and until the noise power integrated into critical bands (using CR data from Johnson et al., 1989) fell below the audiogram at all frequencies. This was assumed to be the range at which the noise would no longer be audible and, hence, no longer able to mask even the quietest signals. Therefore, RL is plotted over a range of 38 km, the ship's range of audibility. It is worth noting that the range of audibility differs for listeners with different hearing characteristics (e.g., audiogram, CR). In the maskogram, a calling beluga whale is located along the diagonal (red line). A listening whale can be anywhere in the plot and is indicated by the white face. Various distances can be read off the x-axis. The ship-to-listener distance (white arrow) is the sum of the ship-to-caller distance (black arrow) and the caller-to-listener distance (yellow arrow) in this situation, where the caller is in between the ship and the listener.

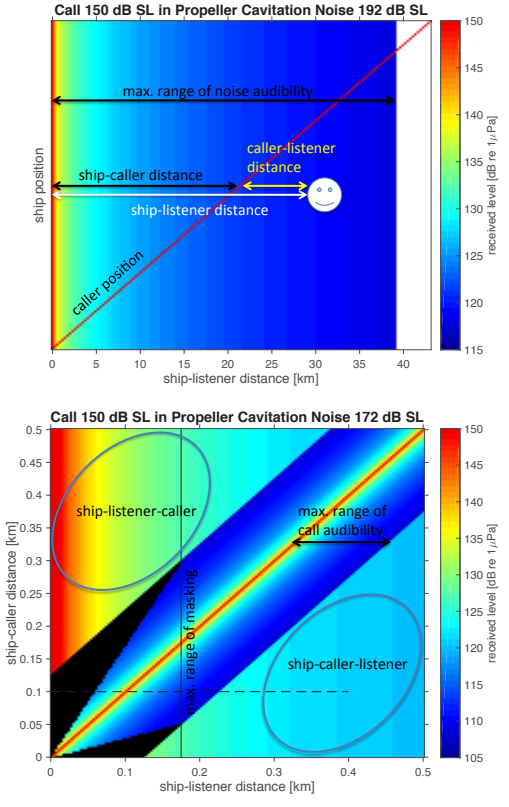

Figure 2. Positions of noise source, calling animal, and listening animal in a maskogram (top), and ranges of audibility and masking for the example of a beluga listening to another beluga in the presence of a ship (bottom). The bottom panel is a zoomed-in version of the top panel at lower ship source level (SL). Left of the diagonal, the distance between the ship and the listener is less than the distance between the ship and the caller. Right of the diagonal, the distance between the ship and the listener is greater than the distance between the ship and the caller. The received level (RL) of the ship at all listener positions is plotted in the background. The RL of the call is plotted along the diagonal wherever the call is deemed audible above the ship noise. In the black area, the call is expected to be masked.

The ship-to-caller distance can also be noted along the y-axis for ease of reading ranges off the maskogram (Figure 2, bottom), where the ship SL was 172 dB re 1 µPa @ 1 m and the call SL 150 dB re 1 µPa @ 1 m. The lower panel (Figure 2) shows a "zoomed-in" version of a maskogram, focusing on close ranges where the zone of masking occurs at the expense of illustrating the longer range of audibility. In the top left corner of the plot, the listener is between the ship and caller. In the bottom right corner of the plot, the caller is between the ship and listener. The broadband RL of the call is plotted along the diagonal. The same colour scale is used for the RL of both the ship and call. The call RL is plotted wherever the call is audible in quiet conditions as measured behaviourally. The maximum range of call detection is modelled to be 120 m. In the black areas, ship noise is expected to mask the call. In other words, this is where the behaviourally measured, critical SNR (over the bandwidth of the call) is not reached. This critical SNR accounts for masking release phenomena such as out-of-band listening and comodulation masking release, but not spatial release from masking as signal and noise were transmitted by the same sound projector during the behavioural experiment. In the absence of direct measurements of masking with complex signals and noises, a CR can be used instead of the critical SNR in accordance with the power spectrum model of masking and additional assumptions for masking release. The maximum range of masking is estimated as 175 m as indicated by the vertical black line. For comparison, where the ship SL is 20 dB higher (see Figure 2, top), the maximum range of masking is 5.1 km, which could be seen if one zoomed into the top plot and looked at the zone of masking at a finer scale (not shown).

Considering the horizontal dashed line (see Figure 2, bottom), a ship would be 100 m from a calling whale. The listening whale could be anywhere along the dashed line. If the listening whale were far away (e.g., 400 m from the ship) at the right end of the x-axis, the listener would hear ship noise at an RL of about 120 dB re 1 µPa. As the listening whale approached the ship, the ship RL would increase. At a range of 220 m from the ship, the listener would hear both the whale and ship, and the ship RL would be greater than the call RL, but the ship noise would not mask the call because the animal would be able to detect enough bits of the call through the quieter gaps in the amplitude-modulated ship noise and also because of the comodulation masking release (Erbe, 2008).

In addition, some of the broadband energy of the ship noise would be outside the band of the call. As the listener got closer to both the ship and caller (still travelling along the dashed line towards the left), the received levels of the ship and caller would increase. At 100 m range from the ship, the listener would be at the same location as the caller, and the call RL would be at a maximum of 150 dB re 1 µPa. The listener would still hear both the call and ship. As the listener moved even closer to the ship, it would leave the caller behind (i.e., the listener would be in between the ship and caller). The ship would get louder, and the call would get quieter. At about 60 m from the

ship and 40 m from the caller (remember the caller would be 100 m from the ship), the listener could only hear the ship. The call would be masked as indicated by the black zone. It would be detectable at this location in the absence of the ship. If the caller were closer to the ship, less than 50 m (i.e., the dashed line drops to 50 m along the y-axis), then there would be two zones of masking—one on the far side of both the ship and caller, and one in between the ship and caller.

There are several features that can be read off the maskogram, including the maximum range of audibility of the ship; the maximum range of audibility of the call; the maximum range of the ship's masking potential; the range of masking as a function of distance between the ship and calling whale; and the variability of the occurrence of masking as a function of ship, caller, and listener position. Further examples based on the behavioural experiments with beluga whales are given (Figure 3). Bubbler system noise at a SL of 185 dB re 1 μPa @ 1 m was modelled audible to beluga whales over a 26-km range (Figure 3a); the maximum range of masking, however, was only just over 3 km for a call with a SL of 150 dB re 1 μPa @ 1 m (Figure 3b). Propeller cavitation noise at the same SL as bubbler system noise was deemed audible over a longer range (28 km; Figure 3c) but masked over a shorter range (1.7 km; Figure 3d).

Considering the regions in Figures 3a through d, where any listener can be in relation to the ship and caller, the area where the ship is expected to be audible is huge compared to the area where the ship might mask the call. The maskogram can easily be extended to negative x, where the ship is between the listener and caller (Figure 3e). On the left side of both the ship and caller, the call would be completely masked in the case of Figure 3e but not in the case of Figure 3f, where the noise SL is less. In Figures 3a through e, there are two zones of masking—one for listeners in between the ship and caller, and one on the right side of the ship and caller. In Figure 3f, there is no masking on the right side of the ship and caller, but only one zone of masking, near the ship.

Communication space can also be calculated from these maskograms. Looking at Figure 3e, if the modelled ship with a SL of 172 dB re 1 μPa @ 1 m passed a calling whale no closer than 300 m, there would be no masking (because the black zone of masking ends at 300 m on the y-axis). If it passed at 40 m from the calling whale (white line in Figure 3e), then, at the point of closest approach, the maskogram shows a cumulative length (ship-listener range) of about 130 m over which a listener could not hear the caller: 20 m on the right (far) side of both the ship and caller, 20 m in between the ship and caller, and another 90 m on the far (left) side of both the ship and caller.

In the absence of ship noise, the caller would be audible over 240 m (i.e., 120 m either side of the caller; see also Figure 2, bottom). Hence, with a ship at 40 m from the calling whale, this whale's communication range would be reduced to about one half. As the ship approached the calling whale from afar, masking would commence at 300-m distance between the ship and the caller. If the closest point of approach were 40 m, the loss of communication space would be equal to the black area for ship-caller distances of 40 to 300 m divided by the area in the maskogram where the whale could be heard in the absence of the ship (i.e., from 40 to 300 m along the y-axis × 240 m along the x-axis [= 260 m × 240 m]). In the worst case, when the ship passes close by the whale (ship-caller distance of 1 m), the ratio of the masked (black) area to the total area of call audition in the absence of the noise gives the percent loss of communication space for the duration of the ship passing the calling whale from +300 m to -300 m: 23%.

In the above calculations, only the relative ranges between the ship and caller and between the ship and listener were considered. The maskograms apply to the case for which the ship, caller, and listener are positioned along one line, or where the ship and caller emit sound omnidirectionally, and the listener's sound reception is omnidirectional at the frequencies of the noise and the call (i.e., any potential angular separation between the ship and caller does not help the listener detect the call in the noise). While there are no data on spatial release from masking in beluga whales for ship noise and beluga calls, masking release of up to 12 dB has been demonstrated in other cetaceans at communication frequencies of several kHz (Zaitseva et al., 1980; Bain & Dahlheim, 1994). The spatial release from masking changes the critical SNR as signal and noise are spatially separated. Assuming a linear decrease in the amount of masking by as much as 0 to -12 dB as the noise rotates from the front to the back of the listening animal that is facing the caller, Figure 4 illustrates how a spatial release from masking can be included in the maskogram and how it affects the extent of the zone of masking.

When defining the angle α as the angle at the listener, between the listener-ship path and the listener-caller path, it is convenient to plot a listener-centred maskogram in which the listener-ship distance is depicted on the x-axis and the listener-caller distance on the y-axis. As a first step, the ship noise is propagated from its source level on the left side of the maskogram, over the listener-ship ranges along the x-axis. Broadband RL are

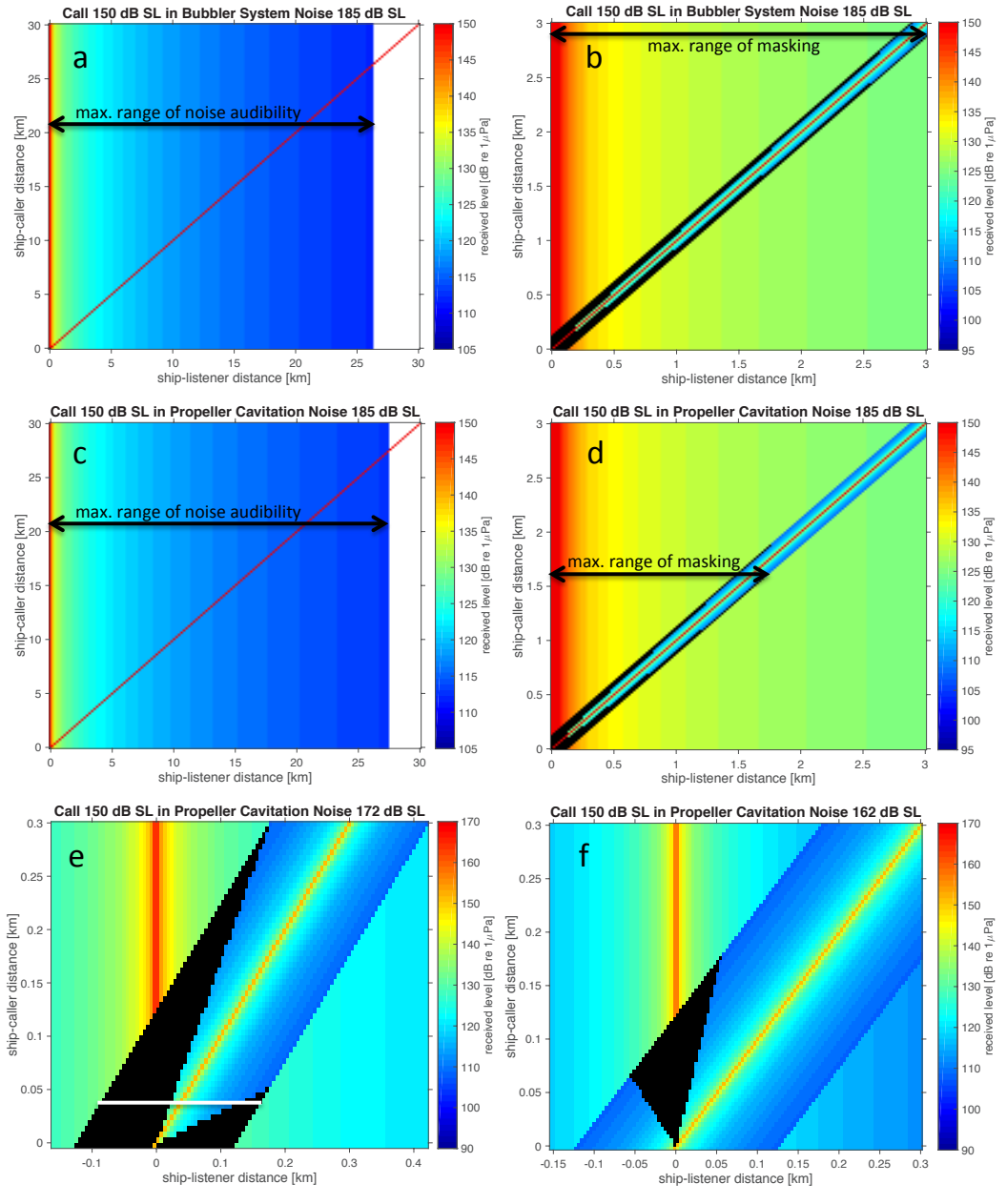

Figure 3. Maskograms of an icebreaker's bubbler system noise and propeller cavitation noise. The source level (SL) of the call was 150 dB re 1 μPa @ 1 m in all examples. The SL of both types of noise was 185 dB re 1 μPa @ 1 m in a through d, and less in e and f. Propeller cavitation noise was modelled audible over longer ranges than bubbler system noise (a, c), yet masked over shorter ranges (b, d). Multiple zones of masking can exist—for example, on the far sides of both ship and caller and in between ship and caller (e, f). If a ship passed a caller to a closest point of approach (CPA) of 40 m (white line in e), the communication space of the caller at this point of approach would be reduced by 50% (ratio of black masked to unmasked length along the white line). In the worst case, where the ship approached to within 1 m, the communication space (integrated over the duration of the pass rather than only at CPA) would be reduced by 23% (computed as the ratio of black area to call audible area in the absence of the ship).

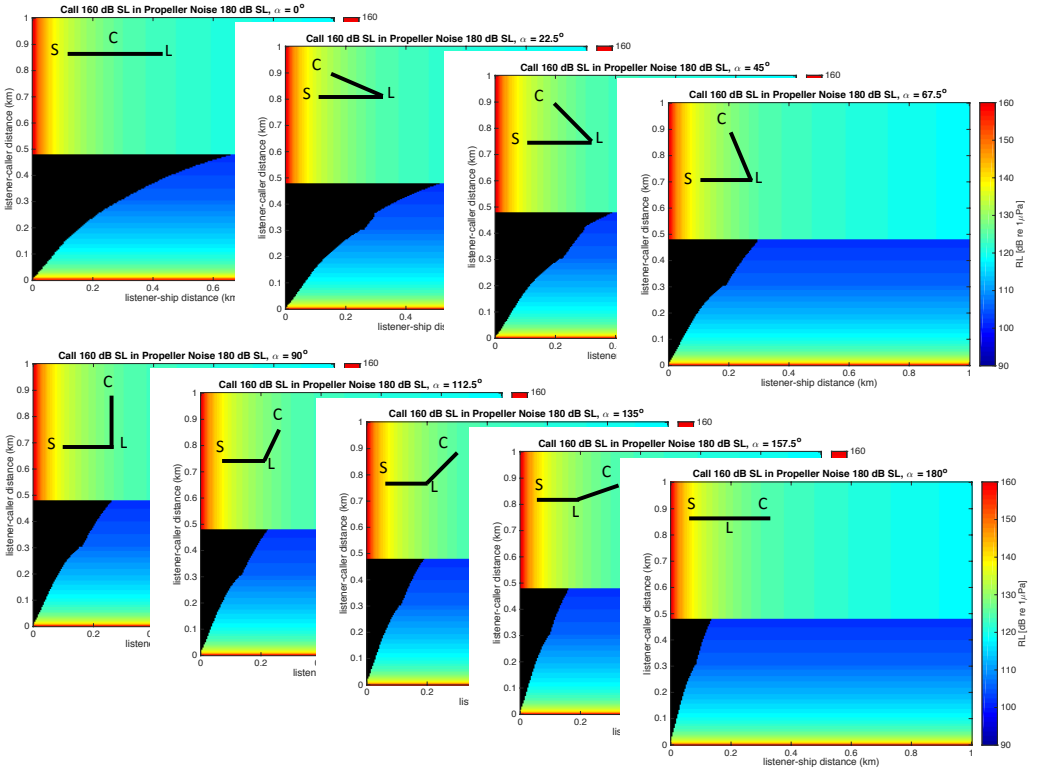

Figure 4. Zones of masking as a function of angular separation between the caller (C) and the masker (ship, S). The plots show a decrease in the zone of masking as the horizontal angle between the directions from the listener (L) to the caller and to the masker increases.

shown as colours in the background. As a second step, the call is propagated from its source level on the bottom of the maskogram, over the listener-call ranges along the y-axis. The broadband call RL are shown as colours in the foreground. Wherever the SNR is less than the threshold measured with the trained beluga whale, plus the spatial release from masking as a function of angle, the area is shaded black. At $\alpha = 0^{o}$, ship, caller, and listener are in a straight line, with the listener on the far side of both the ship and caller. The order of ship and caller can be reversed. On the left side of the diagonal in the maskogram, the ship is closer to the listener than is the caller; on the right side, the caller is closer to the listener than is the ship. At 180°, the listener is in between the ship and caller. As the angular separation between the ship and caller increases, the potential of the noise to mask the call decreases, and the extent of the plotted zone of masking decreases—in this case, by a factor 5 in range (from 670 to 130 m). In all plots, the listener is assumed to face the caller. At 0°, the listener directly faces both the ship and caller. At 180°, the listener faces the caller, and the ship is directly behind the listener.

Discussion

A common approach to predicting masking is a combination of the power spectrum model and the equal-power assumption or the CR (e.g., Erbe & Farmer, 2000; Hatch et al., 2008; Clark et al., 2009; Jensen et al., 2009, 2012; Hermannsen et al., 2014). In the power spectrum model of masking, the power spectra of signal and noise are computed over a window in time, and, hence, the levels are averaged over time, which is why this model fails when the noise has a temporal structure. Masking release mechanisms, such as comodulation masking release and spatial release from masking, aid in signal detection and are not captured by the power spectrum model. The amount of masking release can be significant (Zaitseva et al., 1980; Holt & Schusterman, 2007;

Branstetter et al., 2013b). The maskograms shown in this paper can help illustrate the effects of some of these processes.

The maskograms can be based on the power spectrum model of masking in which masking is considered to happen wherever the signal level is less than the appropriate CR for that species above the noise power spectral density level. However, it would be important in such cases to outline the assumptions used in the creation of the maskogram, including which masking release mechanisms were or were not applied and why.

Ideally, the maskograms would be populated with realistic data about signal and noise properties and measures of masking release obtained from laboratory psychophysical experiments. The example maskograms presented in this paper were based on behavioural experiments using recorded ship noise and beluga calls; masking was determined to happen whenever the signal level was less than a critical SNR below the noise level. These critical SNRs were computed over the full bandwidth of the call and represent the mean SNR at which the animal responded out of all signal-and-noise presentations with variable relative time lags between signal and noise.

Even though the two types of noise included herein had the same bandwidth and root-mean-square sound pressure level, bubbler system noise was temporally continuous, while propeller cavitation noise was amplitude modulated across multiple bands. The critical SNR was 4 dB less for propeller cavitation noise than bubbler system noise (Erbe, 2000). Some, but not all, of the known anti-masking processes possessed by mammals in general and probably belugas as well, such as comodulation masking release (Branstetter & Finneran, 2008; Trickey et al., 2010; Cunningham et al., 2014), within-valley listening (Branstetter et al., 2013b), multiple looks (Erbe, 2008), and high within-call redundancy, are expected to have affected the whale's performance and, hence, are assumed to be indirectly included in the critical SNR. The resulting zone of masking is, therefore, less than what would be predicted by an equal-power or CR approach but could still overpredict actual masking if tested in the field for the reasons that follow.

A spatial release from masking was not studied in the beluga experiment but was demonstrated in the maskograms for conceptual purposes, reducing the zone of masking. The listener was modelled to orientate towards and focus on the caller. In the wild, this might not always be the case. Additional anti-masking strategies can be employed by the caller—for example, the Lombard effect, wherein the caller raises the level of the emitted call in relation to background noise (Scheifele et al., 2005; Holt et al., 2009), reducing the potential for masking. Natural, biotic, and abiotic noise can also result in masking, and the Lombard response was shown in humpback whales (*Megaptera novaeangliae*) as a response to wind noise (Dunlop et al., 2014).

Natural ambient noise in many parts of the world's oceans, including the Arctic, can be considerable, and masking by thermal ice-cracking noise was studied in the behavioural experiments as well (Erbe & Farmer, 1998; Erbe, 2000). This noise had the weakest masking potential, likely due to its intermittency, providing ample opportunity to detect the signal from parts emerging through gaps in the noise. In different, more continuous background noises at a higher level, ambient noise will affect the masking by anthropogenic noise in the sense that the ranges of audibility of both the call and anthropogenic noise will be less (Kastelein et al., 2011). The effect of ambient noise can be included in the maskogram and would show a reduction in the extent of the potential zone of masking.

Whether the maskogram is based on a simple power spectrum model or behavioural measurements with specific, recorded signal and noise, it is useful to illustrate the effects of various parameters and masking release mechanisms and to estimate the extent of the zone of masking. The maskogram is an illustration tool and not a model for the masking process. Results from masking experiments with realistic signals and noise can feed into maskograms, let us challenge existing models, aid our understanding of masking release phenomena in real-life situations, and let us derive parameters and concepts that can inform and ultimately improve masking models.

Acknowledgments

The development of the maskogram was sponsored by the Canadian Coast Guard. The beluga masked hearing experiments that are cited in this paper and on which the maskogram examples are based were carried out at the Vancouver Aquarium, and I am grateful for the advice, help, and support received from the Aquarium, its whale trainers, and, specifically, John Ford. Thank you also to my former colleagues at the Institute of Ocean Sciences, British Columbia, Canada, specifically David Farmer, and at the Department of Earth, Ocean and Atmospheric Sciences, the University of British Columbia, specifically Matthew Yedlin. Finally, I wish to thank three anonymous reviewers for their unusually detailed, careful, and constructive comments on the manuscript.

Literature Cited

Ainslie, M. A., & McColm, J. G. (1998). A simplified formula for viscous and chemical absorption in sea water. *The Journal of the Acoustical Society of America*, *103*(3), 1671-1672. http://dx.doi.org/10.1121/1.421258

Au, W. W. L. (1993). *The sonar of dolphins*. New York: Springer-Verlag.

Au, W. W. L., & Moore, P. W. B. (1990). Critical ratio and critical bandwidth for the Atlantic bottlenose dolphin. *The Journal of the Acoustical Society of America*, *88*(3), 1635-1638. http://dx.doi.org/10.1121/1.400323

Bain, D., & Dahlheim, M. (1994). Effects of masking noise on detection thresholds of killer whales. In T. Loughlin (Ed.), *Marine mammals and the Exxon Valdez* (pp. 243-256). San Diego: Academic Press.

Branstetter, B. K., & Finneran, J. J. (2008). Comodulation masking release in bottlenose dolphins (*Tursiops truncatus*). *The Journal of the Acoustical Society of America*, *124*(1), 625-633. http://dx.doi.org/10.1121/1.2918545

Branstetter, B. K., Trickey, J. S., Aihara, H., Finneran, J. J., & Liberman, T. R. (2013a). Time and frequency metrics related to auditory masking of a 10 kHz tone in bottlenose dolphins (*Tursiops truncatus*). *The Journal of the Acoustical Society of America*, *134*(6), 4556-4565. http://dx.doi.org/10.1121/1.4824680

Branstetter, B. K., Trickey, J. S., Bakhtiari, K., Black, A., Aihara, H., & Finneran, J. J. (2013b). Auditory masking patterns in bottlenose dolphins (*Tursiops truncatus*) with natural, anthropogenic, and synthesized noise. *The Journal of the Acoustical Society of America*, *133*(3), 1811-1818. http://dx.doi.org/10.1121/1.4789939

Clark, C. W., Ellison, W. T., Southall, B. L., Hatch, L., Van Parijs, S. M., Frankel, A., & Ponirakis, D. (2009). Acoustic masking in marine ecosystems: Intuitions, analysis, and implication. *Marine Ecology Progress Series*, *395*, 201-222. http://dx.doi.org/10.3354/Meps 08402

Cunningham, K. C., Southall, B. L., & Reichmuth, C. (2014). Auditory sensitivity in complex listening scenarios. *The Journal of the Acoustical Society of America*, *136*(6), 3410-3421. http://dx.doi.org/10.1121/1.4900568

Cure, C., Antunes, R., Alves, A. C., Visser, F., Kvadsheim, P. H., & Miller, P. J. O. (2013). Responses of male sperm whales (*Physeter macrocephalus*) to killer whale sounds: Implications for anti-predator strategies. *Scientific Reports*, *3*, 1579. http://dx.doi.org/10.1038/srep01579

Dooling, R. J., & Blumenrath, S. H. (2014). Avian sound perception in noise. In H. Brumm (Ed.), *Animal communication in noise* (pp. 229-250). Heidelberg, Germany: Springer Verlag.

Dunlop, R. A., Cato, D. H., & Noad, M. J. (2014). Evidence of a Lombard response in migrating humpback whales (*Megaptera novaeangliae*). *The Journal of the Acoustical Society of America*, *136*(1), 430-437. http://dx.doi.org/10.1121/1.4883598

Erbe, C. (2000). Detection of whale calls in noise: Performance comparison between a beluga whale, human listeners and a neural network. *The Journal of the Acoustical Society of America*, *108*(1), 297-303. http://dx.doi.org/10.1121/1.429465

Erbe, C. (2008). Critical ratios of beluga whales (*Delphinapterus leucas*) and masked signal duration. *The Journal of the Acoustical Society of America*, *124*(4), 2216-2223. http://dx.doi.org/10.1121/1.2970094

Erbe, C. (2012). The effects of underwater noise on marine mammals. In A. N. Popper & A. D. Hawkins (Eds.), *The effects of noise on aquatic life* (pp. 17-22). *Advances in Experimental Medicine and Biology*, *730*. New York: Springer Verlag.

Erbe, C., & Farmer, D. M. (1998). Masked hearing thresholds of a beluga whale (*Delphinapterus leucas*) in icebreaker noise. *Deep-Sea Research Part II*, *45*(7), 1373-1388. http://dx.doi.org/10.1016/S0967-0645(98)00027-7

Erbe, C., & Farmer, D. M. (2000). A software model to estimate zones of impact on marine mammals around anthropogenic noise. *The Journal of the Acoustical Society of America*, *108*(3), 1327-1331. http://dx.doi.org/10.1121/1.1288938

Fletcher, H. (1940). Auditory patterns. *Reviews of Modern Physics*, *12*, 47-65.

Gannon, D. P., Barros, N. B., Nowacek, D. P., Read, A. J., Waples, D. M., & Wells, R. S. (2005). Prey detection by bottlenose dolphins, *Tursiops truncatus*: An experimental test of the passive listening hypothesis. *Animal Behaviour*, *69*, 709-720. http://dx.doi.org/10.1016/j.anbehav.2004.06.020

Gaspard III, J. C., Bauer, G. B., Reep, R. L., Dziuk, K., Cardwell, A., Read, L., & Mann, D. A. (2012). Audiogram and auditory critical ratios of two Florida manatees (*Trichechus manatus latirostris*). *Journal of Experimental Biology*, *215*(9), 1442-1447. http://dx.doi.org/10.1242/jeb.089201

Ghoul, A., & Reichmuth, C. (2014). Hearing in the sea otter (*Enhydra lutris*): Auditory profiles for an amphibious marine carnivore. *Journal of Comparative Physiology A*, *200*(11), 967-981. http://dx.doi.org/10.1007/s00359-014-0943-x

Hatch, L., Clark, C., Merrick, R., Van Parijs, S., Ponirakis, D., Schwehr, K., . . . Wiley, D. (2008). Characterizing the relative contributions of large vessels to total ocean noise fields: A case study using the Gerry E. Studds Stellwagen Bank National Marine Sanctuary. *Environmental Management*, *42*(5), 735-752. http://dx.doi.org/10.1007/s00267-008-9169-4

Hermannsen, L., Beedholm, K., Tougaard, J., & Madsen, P. T. (2014). High frequency components of ship noise in shallow water with a discussion of implications for harbor porpoises (*Phocoena phocoena*). *The Journal of the Acoustical Society of America*, *136*(4), 1640-1653. http://dx.doi.org/10.1121/1.4893908

Herzing, D. L. (1996). Vocalizations and associated underwater behaviour of free-ranging Atlantic spotted

dolphins, *Stenella frontalis* and bottlenose dolphins, *Tursiops truncatus*. *Aquatic Mammals*, *22*(2), 61-79.

Holt, M. M., & Schusterman, R. J. (2007). Spatial release from masking of aerial tones in pinnipeds. *The Journal of the Acoustical Society of America*, *121*(2), 1219-1225. http://dx.doi.org/10.1121/1.2404929

Holt, M. M., Noren, D. P., Veirs, V., Emmons, C. K., & Veirs, S. (2009). Speaking up: Killer whales (*Orcinus orca*) increase their call amplitude in response to vessel noise. *The Journal of the Acoustical Society of America*, *125*(1), El27-El32. http://dx.doi.org/10.1121/1.3040028

Jensen, F., Beedholm, K., Wahlberg, M., Bejder, L., & Madsen, P. (2012). Estimated communication range and energetic cost of bottlenose dolphin whistles in a tropical habitat. *The Journal of the Acoustical Society of America*, *131*(1), 582-592. http://dx.doi.org/10.1121/1.3662067

Jensen, F. H., Bejder, L., Wahlberg, M., Aguilar de Soto, N., Johnson, M., & Madsen, P. T. (2009). Vessel noise effects on delphinid communication. *Marine Ecology Progress Series*, *395*, 161-175. http://dx.doi.org/10.3354/Meps 08204

Johnson, C. S. (1968). Masked tonal thresholds in a bottlenose porpoise. *The Journal of the Acoustical Society of America*, *44*(4), 965-967. http://dx.doi.org/10.1121/1.1911236

Johnson, C. S., McManus, M. W., & Skaar, D. (1989). Masked tonal hearing thresholds in the beluga whale. *The Journal of the Acoustical Society of America*, *85*(6), 2651-2654. http://dx.doi.org/10.1121/1.397759

Kastelein, R. A., Steen, N., de Jong, C., Wensveen, P. J., & Verboom, W. C. (2011). Effect of broadband-noise masking on the behavioral response of a harbor porpoise (*Phocoena phocoena*) to 1-s duration 6-7 kHz sonar up-sweeps. *The Journal of the Acoustical Society of America*, *129*(4), 2307-2315. http://dx.doi.org/10.1121/1.3559679

Kastelein, R. A., Wensveen, P. J., Hoek, L., Au, W. W. L., Terhune, J. M., & de Jong, C. A. F. (2009). Critical ratios in harbour porpoises (*Phocoena phocoena*) for tonal signals between 0.315 and 150 kHz in random Gaussian white noise. *The Journal of the Acoustical Society of America*, *126*(3), 1588-1597. http://dx.doi.org/10.1121/1.3177274

Lucke, K., Lepper, P. A., Hoeve, B., Everaarts, E., van Elk, N., & Siebert, U. (2007). Perception of low-frequency acoustic signals by a harbour porpoise (*Phocoena phocoena*) in the presence of simulated offshore wind turbine noise. *Aquatic Mammals*, *33*(1), 55-68. http://dx.doi.org/10.1578/AM.33.1.2007.55

Moore, B. C. (Ed.). (1995). *Hearing*. San Diego: Academic Press.

Richardson, W. J., Greene, C. R., Jr., Malme, C. I., & Thomson, D. H. (1995). *Marine mammals and noise*. San Diego: Academic Press.

Scheifele, P. M., Andrew, S., Cooper, R. A., Darre, M., Musiek, F. E., & Max, L. (2005). Indication of a Lombard vocal response in the St. Lawrence River beluga. *The Journal of the Acoustical Society of America*, *117*(3), 1486-1492. http://dx.doi.org/10.1121/1.1835508

Southall, B. L., Schusterman, R. J., & Kastak, D. (2000). Masking in three pinnipeds: Underwater, low-frequency critical ratios. *The Journal of the Acoustical Society of America*, *108*(3), 1322-1326. http://dx.doi.org/10.1121/1.1288409

Southall, B. L., Schusterman, R. J., & Kastak, D. (2003). Auditory masking in three pinnipeds: Aerial critical ratios and direct critical bandwidth measurements. *The Journal of the Acoustical Society of America*, *114*(3), 1660-1666. http://dx.doi.org/10.1121/1.1587733

Trickey, J. S., Branstetter, B. K., & Finneran, J. J. (2010). Auditory masking of a 10 kHz tone with environmental, comodulated, and Gaussian noise in bottlenose dolphins (*Tursiops truncatus*). *The Journal of the Acoustical Society of America*, *128*(6), 3799-3804. http://dx.doi.org/10.1121/1.3506367

Turnbull, S. D. (1994). Changes in masked thresholds of a harbor seal *Phoca vitulina* associated with angular separation of signal and noise sources. *Canadian Journal of Zoology*, *72*, 1863-1866. http://dx.doi.org/10.1139/z94-253

Turnbull, S. D., & Terhune, J. M. (1990). White noise and pure tone masking of pure tone thresholds of a harbour seal listening in air and underwater. *Canadian Journal of Zoology*, *68*, 2090-2097. http://dx.doi.org/10.1139/z90-291

Tyack, P. L. (1998). Acoustic communication under the sea. In S. L. Hopp, M. J. Owren, & C. S. Evans (Eds.), *Animal acoustic communication* (pp. 163-220). Berlin: Springer-Verlag.

Zaitseva, K. A., Akopian, A. I., & Morozov, V. P. (1975). Noise resistance of the dolphin auditory analyzer as a function of noise direction. *Biofizika*, *20*(3), 519-521.

Zaitseva, K. A., Morozov, V. P., & Akopian, A. I. (1980). Comparative characteristics of spatial hearing in the dolphin *Tursiops truncatus* and man. *Neuroscience and Behavioral Physiology*, *14*(1), 80-83. http://dx.doi.org/10.1007/BF01148460